RESEARCH ARTICLE | DECEMBER 13 2024

Controllable droplet velocity: Exploration of droplet transport based on discharge plasma

Dingchen Li (李丁晨); Chuan Li (李传); Tingyu Liang (梁廷玉); Jiawei Li (李家玮); Zhiwen Yang (杨志文); Qixiong Fu (傅琦雄); Ming Zhang (张明); Yong Yang (杨勇); Kexun Yu (于克训); Yaping Du (杜亚平); Xiangen Zhao (赵贤根)

Physics of Fluids 36, 122020 (2024)
https://doi.org/10.1063/5.0244478

Physics of Fluids ARTICLE pubs.aip.org/aip/pof

Controllable droplet velocity: Exploration of droplet transport based on discharge plasma

Cite as: Phys. Fluids **36**, 122020 (2024); doi: 10.1063/5.0244478
Submitted: 19 October 2024 · Accepted: 25 November 2024 ·
Published Online: 13 December 2024

Dingchen Li (李丁晨),[1,2] Chuan Li (李传),[1,a)] Tingyu Liang (梁廷玉),[1] Jiawei Li (李家玮),[1] Zhiwen Yang (杨志文),[1] Qixiong Fu (傅琦雄),[1] Ming Zhang (张明),[1] Yong Yang (杨勇),[1] Kexun Yu (于克训),[1] Yaping Du (杜亚平),[2] and Xiangen Zhao (赵贤根)[2]

AFFILIATIONS

[1]State Key Laboratory of Advanced Electromagnetic Engineering and Technology, School of Electrical Engineering and Electronics, Huazhong University of Science and Technology, Wuhan 430074, China
[2]Department of Building Environment and Energy Engineering, The Hong Kong Polytechnic University, Hong Kong 999077, China

[a)]Author to whom correspondence should be addressed: lichuan@hust.edu.cn

ABSTRACT

Droplet transport assumes a crucial role in domains such as atmospheric governance, water resource development, drug delivery, medical analysis and detection, as well as the development of biosensors. Currently, droplet transport is accomplished through established chemical environments and structural gradients, yet it fails to precisely control the motion state of droplets. This paper presents an innovative approach for transporting droplets by means of discharge plasma, which governs the start, stop, and velocity of the droplets by modulating the discharge power. We employ discharge plasma to charge and polarize droplets and form gradient electric fields and gradient charges in space for driving droplets. Eventually, we achieved directional transport of diverse droplets via this method, which holds significant potential application value for controlling droplet motion.

I. INTRODUCTION

Droplet directed transport refers to the process of controlling the movement of droplets along a predetermined direction on a solid surface or other medium using physical, chemical, or biological methods under specific conditions.[1–8] As a key technology for precise control of liquid micro movement, droplet directed transport has demonstrated its unique application potential and scientific value in multiple cutting-edge fields such as biomedicine, microfluidics, energy conversion, and environmental engineering.[9]

Presently, the typical approach to achieve the directional transport of droplets is by fabricating chemical or geometric gradients on the medium's surface.[10–15] For instance, Wu *et al.* introduced a hydrophobic/hydrophilic nanofiber membrane with directional hydrophobicity, enabling the directional movement of droplets from hydrophobic to hydrophilic regions.[1] Feng *et al.* employed tip-induced droplet inversion for continuous directional transport at asymmetric tips.[3] Li *et al.* proposed a high-temperature Janus droplet transport method mediated by structural morphology, breaking the symmetric wettability and favoring movement toward areas with high heat transfer coefficients.[16] Li *et al.* developed a novel liquid diode that converts excess surface energy into kinetic energy to propel droplets by advancing their edges.[17] Sun *et al.* reported a high-speed droplet transport method via charge gradient formation through contact with superhydrophobic surfaces.[18] Wang *et al.* achieved droplet self-transfer on a polyimide film by injecting a lubricant using a femtosecond laser.[19] However, a significant drawback of these existing methods is the inability to dynamically adjust the established chemical or geometric setups, leading to an incapability of precisely controlling the droplet transport speed. This fixed transport speed can cause inefficiencies in liquid transportation, such as reduced accuracy, droplet blockages, uneven mixing, and wastage of the carrier solution.

This paper reports a method of directional transport of droplets through discharge plasma, which controls the transport speed of the droplets by adjusting the discharge parameters. This novel method provides an innovative solution for applications that require directional transport of droplets.

II. RESULTS AND DISCUSSION

A. Concept of transmitting droplets by plasma

In accordance with the principle of driving droplet motion, the currently predominant droplet driving approach is to exert a driving force in a fixed direction upon the droplet via chemical or structural gradients. The inability to achieve the dynamic adjustment of droplet transport speed results from the incapability of the operator to manipulate the chemical and structural gradients, thereby resulting in the failure to modify the driving force of the droplet. Hence, the key for attaining droplet velocity regulation lies in the dynamic control of the factors constituting the driving force of the droplet.

In contrast to traditional droplet transport approaches, we positioned the droplets within the discharge plasma region and observed that they were capable of rapid and directional movement on the electrode [Fig. 1(a)]. In our previous research, even when the electrode was perpendicular to the horizontal line, droplets tended to move from top to bottom, as depicted in Figs. 1(b)–1(d).[20] This implies that our discoveries possess stability and universality.

How to control the speed of droplet transport? Based on previous analyses, it is requisite to dynamically regulate the factors that contribute to the formation of the droplet driving force in order to accomplish this objective. Herein, we propose a methodology that discards traditional chemical and structural gradients and employs discharge plasma to form charges and electric field gradients for driving droplets, as depicted in Fig. 1(e). The aforementioned two gradients will, respectively, exert Coulomb force and electric field force on the droplet, and the directions are consistent. By manipulating discharge parameters such as voltage and input power, the gradient distribution can be modified to achieve control over the droplet transport speed.

B. Droplet transport environment

Here, we employ mutually perpendicular sheet electrodes to form an electric field and charge gradient through DC (direct current) corona discharge. As depicted in Fig. 2(a), the droplet enters the corona discharge area and is initially charged by the impact of space charges. Given that the volume of droplets during directional transport is significantly larger than 0.5 μm, the charging mechanism of droplets is typically field-induced charging. The amount of electric charge induced by the field is[21–23]

$$q_s = 3\pi d_p^2 \varepsilon_0 E. \quad (1)$$

Charged droplets will undergo polarization in non-uniform electric fields. Taking positive corona discharge as an instance, negative charges within a droplet are attracted by an electric field and accumulate above the droplet, whereas positive charges are repelled by the electric field and situated below the droplet.

Owing to the intricate electromagnetic environment adjacent to corona discharge, it proves arduous to measure the electric field gradient and charge gradient through experiments.[24–28] Hence, we employed a finite element model to simulate the corona discharge of the sheet electrode, as depicted in Fig. 2(b). The simulation results reveal that corona discharge can efficaciously generate electric fields and charge gradients in space, as shown in Fig. 2(c). In the positive corona discharge space, positive ions pervade the entire space because of the migration effect of the electric field. Positive ions collide with the transfer electrode (ground electrode) under the action of an electric field, generating secondary electrons. Consequently, negative charges will accumulate on the surface of the transmission electrode. Due to the non-uniformity of the corona discharge electric field, the electric field attenuates from both sides directly below the discharge electrode, forming an electric field gradient, as indicated by the purple line in Fig. 2(d). The electric field gradient will also lead to a gradient in the migration speed of positive ions, resulting in the formation of a negative charge gradient on the surface that transfers charges, as shown by the red and blue lines in Fig. 2(d). We regulate the electrode spacing H and input voltage V to control the electric field and charge gradient.

C. Exploration of droplet transport mechanism

With the aim of exploring how plasma can effectuate the directional transport of droplets and regulate the transport speed of

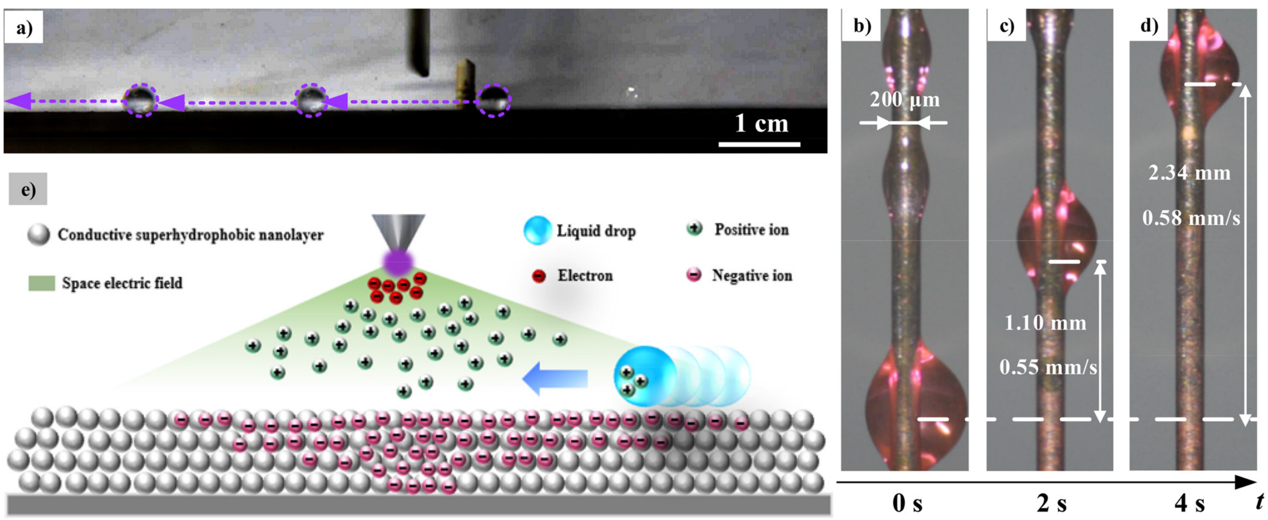

FIG. 1. Droplet transport by discharge plasma. (a) The delayed trajectory of droplets on transport electrode decorated with a superhydrophobic layer; (b)–(d) photos of droplet backflow achieved by discharge plasma[20] (Reproduced with permission from Z. Wang *et al.*, Plasma Source Sci. Technol. **31**, 035007 (2022). Copyright 2022 IOP Science); and (e) schematic diagram of the principle of transporting droplets by discharge plasma.

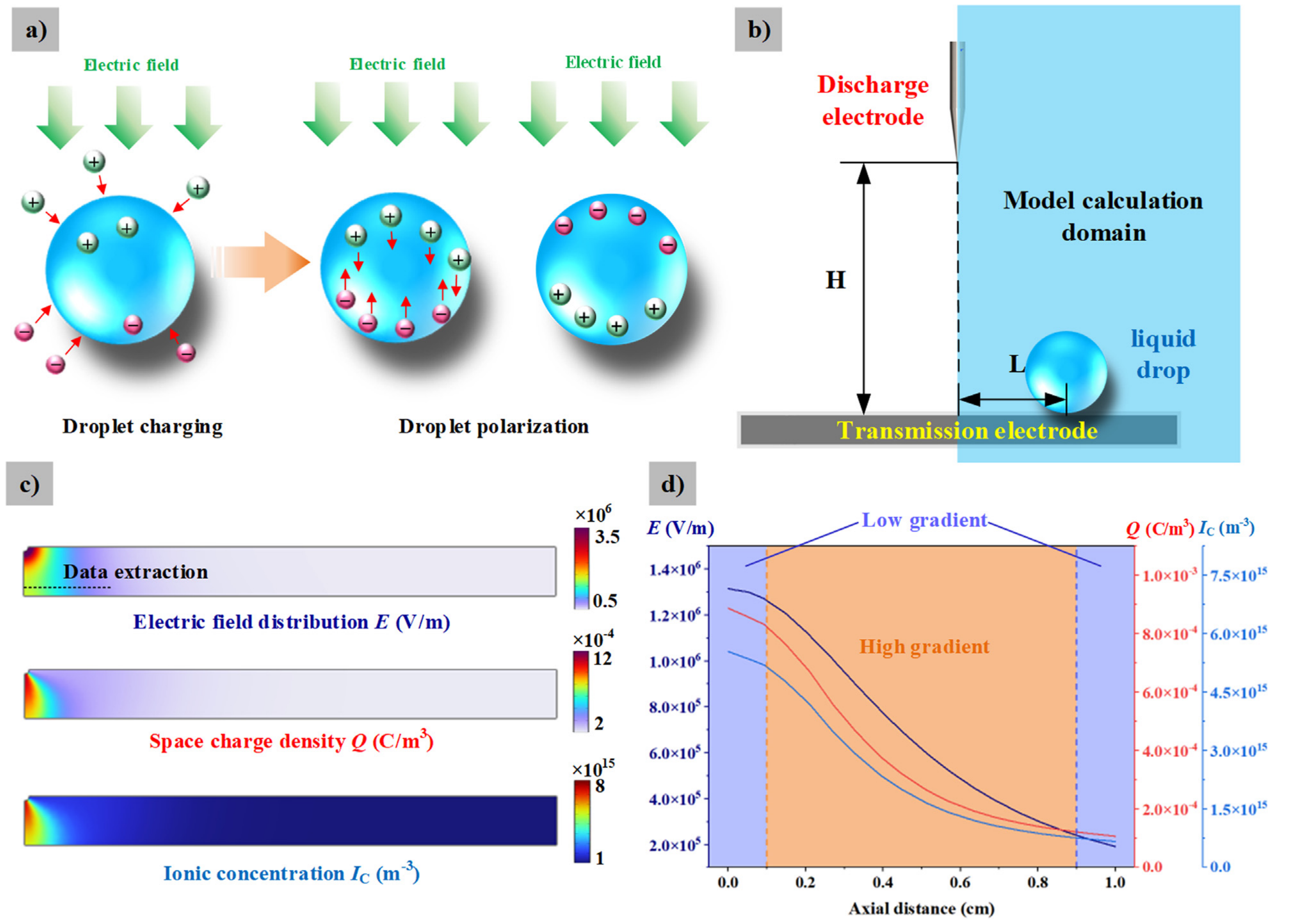

FIG. 2. Characteristics of droplet charging and polarization, spatial electric field, and spatial charge distribution in discharge plasma. (a) Schematic diagram of the droplet field-induced charging and polarization; (b) computational domain for simulating the discharge characteristics of transmission electrodes; (c) cloud map of electric field, space charge, and ion distribution in the discharge area of the transmission electrode; and (d) the electric field E, charge Q, and ion concentration I_c gradient near the transmission electrode.

droplets, we analyzed and deliberated upon the outcomes of droplet transport experiments. The plasma droplet transport platform is depicted in Fig. 3(a). The main body of the experimental platform consists of mutually perpendicular sheet electrodes. The surface of the transmission electrode is coated with a conductive superhydrophobic layer, as illustrated in Fig. 3(b). The contact angle of the droplet is approximately 135°, as presented in Fig. 3(c). Figures 3(d)–3(h) show the position of a 20 μL droplet on the transmission electrode at different times when it is transported by plasma. At 0–60 ms, the droplet is charged and polarized. Beyond 60 ms, the droplet commences to move forward under the action of electrostatic and electric forces. At 160–360 ms, the droplet traverses the discharge electrode toward the other side. We recorded the motion of droplets of different volumes with a camera, as shown in Fig. 4 (multimedia available online). Under the same electrical parameters, the volume of the droplet seems to have an effect on the motion speed.

In Fig. 5, supposing that the charge on the transfer electrode is a point charge, the electrostatic force of the droplet can be expressed as $F_{se} = (\varepsilon_r - 1)\varepsilon_0 k d_p$. Wherein, ε_r is the relative dielectric constant of the droplet, ε_0 is the dielectric constant of the gap, and k is the charge gradient applied to the moving droplet. The electric field force of a droplet can be expressed as $F_e = q_s E$. In accordance with Newton's second law, the transport speed of a droplet is as follows:

$$v = \frac{F_{se} + F_e}{m} t = \frac{6\varepsilon_0}{d_p \rho}\left[\frac{k(\varepsilon_r - 1)}{\pi d_p} + 3\frac{U}{H}\right]. \tag{2}$$

Furthermore, we gauged the starting power [Fig. 5(b)]) and transport speed [Fig. 5(c)]) of the droplets under diverse operating conditions. Herein, we define the "droplet starting power" as the initial discharge power that induces the droplet to move. In Fig. 5(b), the droplet starting power escalates linearly with the horizontal distance L between the droplet and the discharge electrode. The droplet volume V and discharge gap H are both inversely proportional to the droplet starting power. In other words, we employ a large gap electrode to convey larger droplets that demand greater power. As depicted in Fig. 5(c), the variational law of the transport speed of the droplet with the initial position of the droplet is contrary to the starting power, manifesting a linear decrease. We have discerned an interesting phenomenon that when the discharge gap is large, the driving speed of the same droplet is actually higher.

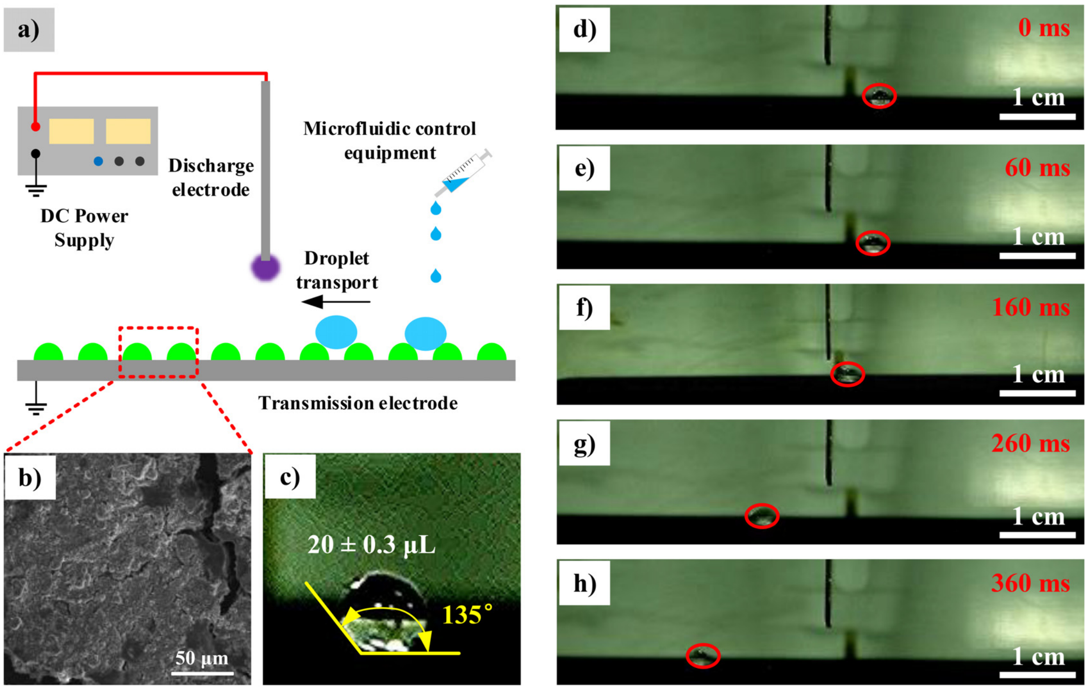

FIG. 3. Experiment on the transmission of droplets by discharge plasma. (a) Droplet transport experimental platform; (b) electron microscopy scanning images of superhydrophobic coatings on transmission electrodes; (c) contact angle of 20 μL droplet on the transmission electrode; and (d)–(h) the position of droplet at different times during discharge plasma transport.

In addition, we have discerned an interesting phenomenon that when the discharge gap is large, the driving speed of the same droplet is actually higher. To explicate this phenomenon, we simulated the corona discharge of electrodes with different gap plates and extracted the electric field and space charge density near the transfer electrode, as shown in Fig. 5(d). We found that when the discharge gap is large, the electric field and space charge are more prone to diverge outward.

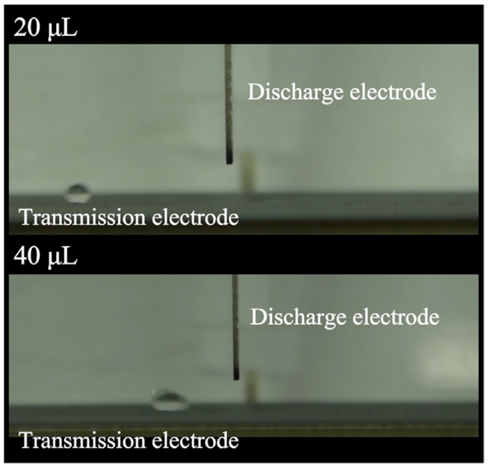

FIG. 4. Droplet transmission of 20 μL and 40 μL by discharge plasma. Multimedia available online.

The aforementioned results engender a higher electric field and space charge density at the initial position of droplets with larger electrode gaps. Therefore, the droplet can acquire greater electrostatic and electric forces.

D. Application examples

As depicted in Fig. 6(a), the discharge plasma can also transport other droplets (50% ethanol was utilized in this study). In this case, we compared the motion velocities of different droplets, as presented in Fig. 6(b). As the initial position of the droplet gradually moves away from the discharge electrode, the velocity of droplet transport also diminishes. The transport velocity of the water droplet is generally higher than that of the 50% ethanol droplet. We contend that the reason for the aforementioned phenomenon is that the conductivity of ethanol is significantly lower than that of water, which is disadvantageous for droplet charging and polarization. The reduction in charge weakens the driving force (electric field force and electrostatic force) of the droplet, resulting in a decrease in droplet velocity.

In the experiment, we also found that when the droplet passes directly below the discharge electrode, the electrode is prone to breakdown. This is caused by the strong electric field formed by polarized droplets and the discharge electrode. Based on this characteristic, a pulsed power supply can be used to achieve continuous transmission of droplets when using plasma to transport them.

In addition, we also discovered in our research that droplets will decelerate after passing through the discharge electrode. This is

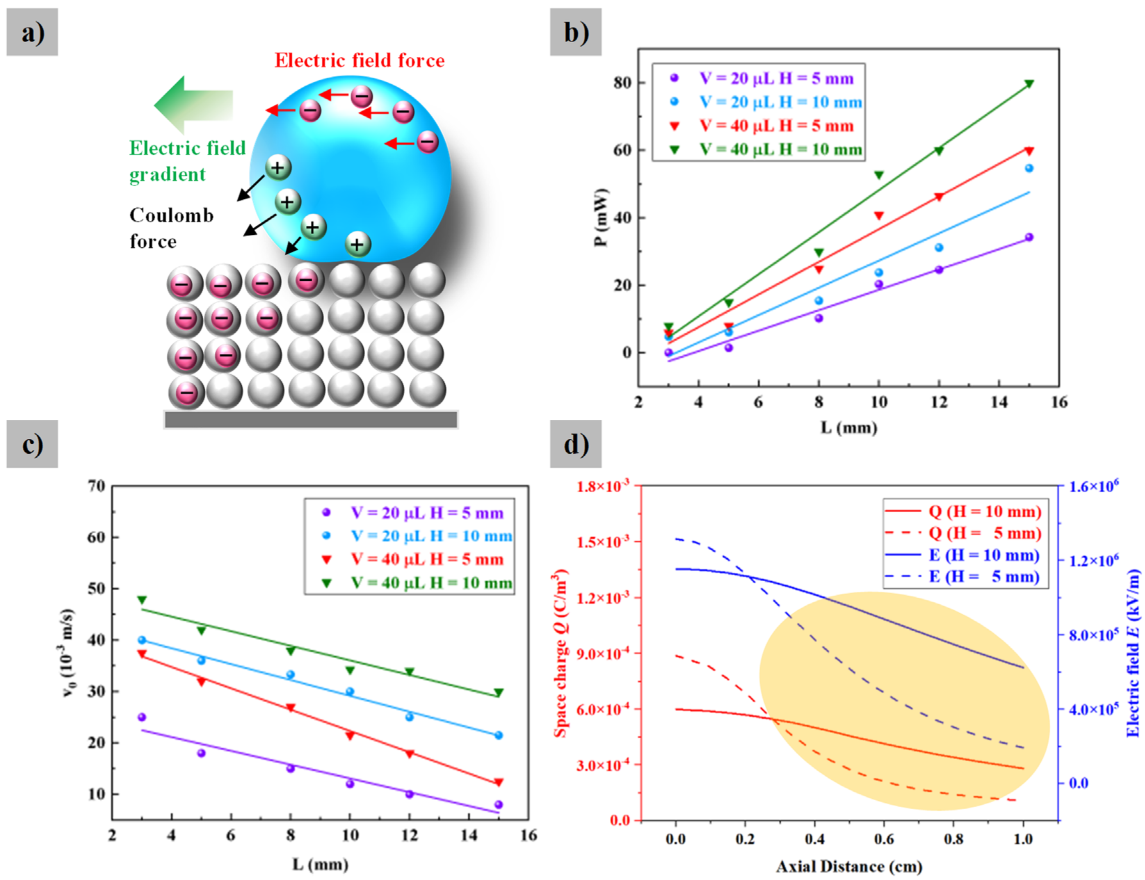

FIG. 5. Transmission mechanism and control of droplet motion characteristics. (a) Schematic diagram of the droplet transport mechanism; (b) the influence of droplet volume (V), electrode gap (H vertical distance between discharge electrode and transfer electrode), and the initial position of the droplet (L distance between droplet and discharge electrode) on the power required for droplet startup; (c) the influence of droplet volume V, electrode gap H, and the initial position of droplet L on the power required for droplet startup; and (d) the distribution of electric field and space charge density during corona discharge of sheet electrodes with different electrode gaps.

because when the droplet traverses the vertical axis of the discharge electrode, its electric field force direction changes from positive (identical to the direction of motion) to negative (contrary to the direction of motion). Based on this finding, we propose a scheme for implementing the long-distance transport of droplets through time-controlled discharge, as shown in Fig. 6(c). Droplets are transported from right to left, and the discharge electrodes can be closed sequentially by a timing switch, causing the droplets to accelerate initially and then decelerate. When the droplet approaches the rear electrode, it is accelerated again. Repeatedly, long-distance transportation of droplets can be accomplished, as shown in Fig. 6(d). We also recorded the continuous transportation of multiple droplets, as shown in Fig. 6(e) (multimedia available online).

The basis for the implementation of this method is to apply Coulomb force and electric field force on the charged droplets and regulate them through electrical parameters. Therefore, the transported droplets must be easily charged and polarized. In addition, the affinity of the transport electrode to the target droplets cannot be too strong to avoid the inability of electricity to overcome it.

In summary, we report a method for transporting droplets via plasma. Contrary to previous methods that relied on structural and chemical gradients, this novel approach can control droplet velocity by regulating input energy. In addition, in the study, we presented application cases of different droplets, confirming the feasibility of plasma-oriented transport of droplets. Our method can pioneer new application avenues for fields such as pharmaceutical analysis and liquid purification that require droplet transport.

In the future, we will further study the effects of different electrode structures and materials on droplet transport, find more optimized electrode designs to improve the control accuracy of electric field and charge gradient, reduce the risk of electrode breakdown, expand the range of experimental parameters, explore the best parameter combination for droplet transport under different voltage, current, frequency, and other conditions, and improve the stability and reliability of the method. In addition, we will strengthen the study of the microscopic mechanism of the interaction between discharge plasma and droplets, deeply analyze the effects of active particles such as electrons, ions, and free radicals in plasma on the surface and internal structure of droplets, and the relationship between these effects and the macroscopic motion characteristics of droplets. Based on a deeper understanding of physics, we aim to improve the existing theoretical model, improve the accuracy of the prediction of droplet transport

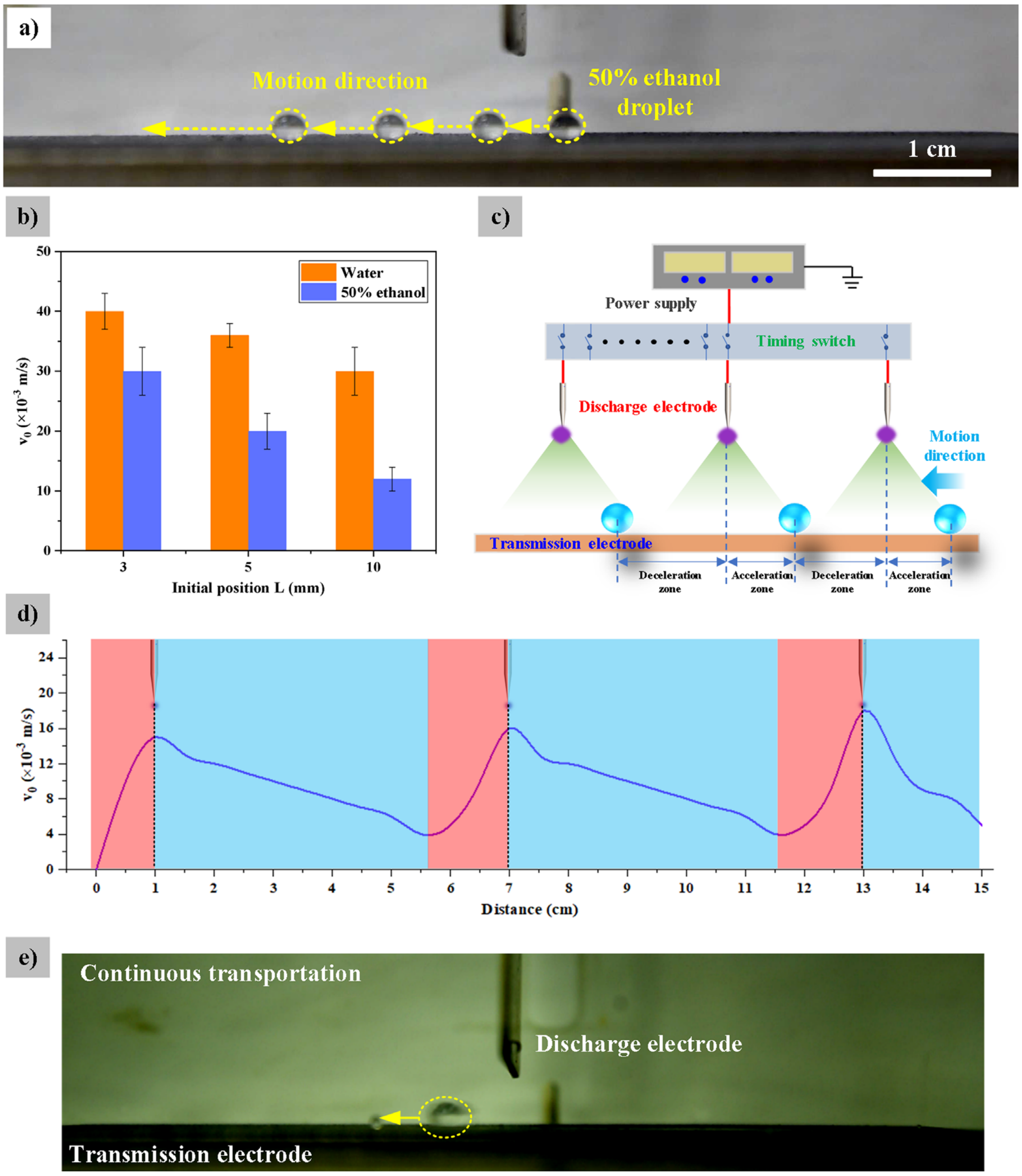

FIG. 6. General application of using discharge plasma to transport droplets. (a) 50% ethanol droplet transport trajectory; (b) transport speed of different droplets; (c) transport speed of different solution droplets; (d) long-distance droplet transport speed varies with spatial position; and (e) continuous transport of multiple droplets via discharge plasma. Multimedia available online.

speed and motion trajectory, and provide a more solid theoretical basis for the optimization and practical application of the method.

ACKNOWLEDGMENTS

This work was supported by the National Natural Science Foundation of China (Grant No. 52207158) and Fundamental Research Funds for the Central Universities (HUST: No. YCJJ20230352).

AUTHOR DECLARATIONS

Conflict of Interest

The authors have no conflicts to disclose.

Author Contributions

Dingchen Li: Conceptualization (lead); Formal analysis (lead); Funding acquisition (lead); Investigation (lead); Methodology (lead);

Validation (lead); Writing – original draft (lead); Writing – review & editing (lead). **Chuan Li:** Conceptualization (equal); Formal analysis (equal); Writing – review & editing (equal). **Tingyu Liang:** Conceptualization (supporting); Investigation (supporting). **Jiawei Li:** Conceptualization (supporting). **Zhiwen Yang:** Conceptualization (supporting). **Qixiong Fu:** Conceptualization (supporting). **Ming Zhang:** Conceptualization (supporting). **Yong Yang:** Conceptualization (supporting). **Kexun Yu:** Data curation (supporting). **Yaping Du:** Data curation (supporting). **Xiangen Zhao:** Data curation (supporting).

DATA AVAILABILITY

The data that support the findings of this study are available from the corresponding author upon reasonable request.

REFERENCES

[1] J. Wu, H. Zhou, H. Wang, H. Shao, G. Yan, and T. Lin, "Novel water harvesting fibrous membranes with directional water transport capability," Adv. Mater. Inter. **6**, 1801529 (2019).
[2] H. Bai, X. Wang, Z. Li, H. Wen, Y. Yang, M. Li, and M. Cao, "Improved liquid collection on a dual-asymmetric superhydrophilic origami," Adv. Mater. **35**, 2211596 (2023).
[3] S. Feng, J. Delannoy, A. Malod, H. Zheng, D. Quéré, and Z. Wang, "Tip-induced flipping of droplets on Janus pillars from local reconfiguration to global transport," Sci. Adv. **6**, eabb4540 (2020).
[4] M. Zhang, D. Li, C. Li, J. Li, P. Wang, Z. Liu, Q. Xu, Y. Yang, K. Yu, B. Zheng, Y. Wang, Y. Liu, and S. Feng, "An electrostatic scheme realizing the complete interception of fog droplets by corona discharge-induced ion wind," J. Phys. D: Appl. Phys. **54**, 255201 (2021).
[5] D. Li, C. Li, J. Li, W. Yang, M. Xiao, M. Zhang, Y. Yang, and K. Yu, "Efficient direction-independent fog harvesting using a corona discharge device with a multi-electrode structure," Plasma Sci. Technol. **24**, 095502 (2022).
[6] D. Li, C. Li, M. Zhang, M. Xiao, J. Li, Z. Yang, Q. Fu, P. Wang, K. Yu, and Y. Pan, "Advanced fog harvesting method by coupling plasma and micro/nano materials," ACS Appl. Mater. Interfaces **16**, 10984 (2024).
[7] M. K. Chaudhury and G. M. Whitesides, "How to make water run uphill," Science **256**, 1539 (1992).
[8] W. Zhou, C. Zhou, H. Yang, J. Wang, J. Du, L. Chen, H. Shen, L. Tan, L. Dong, and X. Zeng, "Janus copper mesh with asymmetric wettability for on-demand oil/water separation and direction-independent fog collection," J. Environ. Chem. Eng. **9**, 105899 (2021).
[9] D. Wang, Q. Sun, M. J. Hokkanen, C. Zhang, F. Y. Lin, Q. Liu, S. P. Zhu, T. Zhou, Q. Chang, B. He, Q. Zhou, L. Chen, Z. Wang, R. H. A. Ras, and X. Deng, "Design of robust superhydrophobic surfaces," Nature **582**, 55 (2020).
[10] A. L. Yarin, W. Liu, and D. H. Reneker, "Motion of droplets along thin fibers with temperature gradient," J. Appl. Phys. **91**, 4751 (2002).
[11] E. S. Kooij, H. P. Jansen, O. Bliznyuk, B. Poelsema, and H. J. W. Zandvliet, "Directional wetting on chemically patterned substrates," Colloids Surf., A **413**, 328 (2012).
[12] Y. Lu, S. Sathasivam, J. Song, F. Chen, W. Xu, C. J. Carmalt, and I. P. Parkin, "Creating superhydrophobic mild steel surfaces for water proofing and oil–water separation," J. Mater. Chem A **2**, 11628 (2014).
[13] D. Haoyu, G. Can, S. Junhan, L. Chuxin, L. Ning, W. Lei, D. Zhichao, and J. Lei, "Controllable high-speed electrostatic manipulation of water droplets on a superhydrophobic surface," Adv. Mater. **31**, e1905449 (2019).
[14] J. Chen, Y. Liu, D. Guo, M. Cao, and L. Jiang, "Under-water unidirectional air penetration via a Janus mesh," Chem. Commun. **51**, 11872 (2015).
[15] L. Hou, N. Wang, X. Man, Z. Cui, J. Wu, J. Liu, S. Li, Y. Gao, D. Li, L. Jiang, and Y. Zhao, "Interpenetrating Janus membrane for high rectification ratio liquid unidirectional penetration," ACS Nano **13**, 4124 (2019).
[16] J. Li, Y. Hou, Y. Liu, C. Hao, M. Li, M. K. Chaudhury, S. Yao, and Z. Wang, "Directional transport of high-temperature Janus droplets mediated by structural topography," Nat. Phys. **12**, 606 (2016).
[17] L. Jiaqian, Z. Xiaofeng, L. Jing, C. Lufeng, Y. Jun, M. Glen, M. K. Chaudhury, and W. Zuankai, "Topological liquid diode," Sci. Adv. **3**, eaao3530 (2017).
[18] Q. Sun, D. Wang, Y. Li, J. Zhang, S. Ye, J. Cui, L. Chen, Z. Wang, H. J. Butt, D. Vollmer, and X. Deng, "Surface charge printing for programmed droplet transport," Nat. Mater. **18**, 936 (2019).
[19] L. Wang, K. Yin, Q. Deng, Q. Huang, J. He, and J. A. Duan, "Wetting ridge-guided directional water self-transport," Adv. Sci. **9**, 2204891 (2022).
[20] Z. Wang, C. Li, M. Xiao, P. Wang, M. Zhang, P. Shi, L. Jiawei, D. Li, F. He, D. W. Yang, Y. Yang, and K. Yu, "Coalescence and counterflow of droplets on needle electrode with negative corona discharge," Plasma Sources Sci. Technol. **31**, 035007 (2022).
[21] M. Damak and K. K. Varanasi, "Electrostatically driven fog collection using space charge injection," Sci. Adv. **4**, eaao5323 (2018).
[22] D. Li, C. Li, J. Li, W. Yang, M. Xiao, M. Zhang, Y. Yang, K. Yu, and Y. Pan, "Efficient corona discharge fog collector: Multiple mesh electrodes with electric field enhances fog harvesting," Plasma Chem. Plasma Process. **42**, 1249 (2022).
[23] D. Li, C. Li, M. Xiao, J. Li, Z. Yang, Q. Fu, M. Zhang, K. Yu, and Y. Pan, "Deconstructing plasma fog collection technology: An experimental study on factors impacting collection efficiency," J. Phys. D: Appl. Phys. **57**, 075201 (2024).
[24] D. Li, C. Li, J. Li, P. Wang, Z. Liu, W. Yang, M. Zhang, Y. Yang, and K. Yu, "Dividing and setting strategy of improving calculation efficiency for needle electrode corona discharge with a large-scale space," High Voltage **7**, 429 (2022).
[25] D. Li, j Li, C. Li, P. Wang, Z. Liu, M. Zhang, Y. Yang, Y. Pan, and K. Yu, "Full-needle geometry: Application in a high-voltage corona discharge model with large-scale space," J. Phys. D: Appl. Phys. **54**, 355202 (2021).
[26] D. Li, C. Li, J. Li, M. Xiao, P. Wang, Z. Liu, M. Zhang, Y. Yang, and K. Yu, "Spatiotemporal corona discharge characteristics of nanoelectrode: Array carbon nanotubes," Plasma Sources Sci. Technol. **32**, 085018 (2023).
[27] D. Li, C. Li, J. Li, W. Yang, M. Xiao, M. Zhang, and K. Yu, "Study on the interaction mechanism of double-blade corona discharge with a large discharge gap," Plasma Sci. Technol. **25**, 045404 (2023).
[28] D. Li, J. Li, C. Li, M. Zhang, P. Wang, Z. Liu, Y. Yang, and K. Yu, "Multi-point discharge model: Study on corona discharge of double-ended needle in large space," Plasma Sci. Technol. **25**, 035402 (2023).